



Discovery of SN 2025wny: A Strongly Gravitationally Lensed Superluminous Supernova at $z = 2.01$

Joel Johansson¹ , Daniel A. Perley² , Ariel Goobar¹ , Jacob L. Wise² , Yu-Jing Qin³ , Zoë McGrath² , Steve Schulze⁴ , Cameron Lemon¹ , Anjasha Gangopadhyay⁵ , Konstantinos Tsalapatas⁵ , Igor Andreoni⁶ , Eric C. Bellm⁷ , Joshua S. Bloom⁸ , Richard Dekany⁹ , Suhail Dhawan¹⁰ , Claes Fransson⁵ , Christoffer Fremling^{9,11} , Matthew J. Graham¹¹ , Steven L. Groom¹² , Daniel Gruen^{13,14} , Xander J. Hall¹⁵ , George Helou¹² , Mansi Kasliwal³ , Russ R. Laher¹² , Ragnhild Lunnan⁵ , Ashish A. Mahabal^{11,16} , Adam A. Miller^{4,17,18} , Edvard Mörtzell¹ , Jakob Nordin¹⁹ , Jacob Osman Hjortlund¹ , R. Michael Rich²⁰ , Reed L. Riddle⁹ , Avinash Singh⁵ , Jesper Sollerman⁵ , Alice Townsend¹⁹ , and Lin Yan⁹

¹ Department of Physics, Oskar Klein Centre, Stockholm University, SE-106 91, Stockholm, Sweden; joeljo@fysik.su.se

² Astrophysics Research Institute, Liverpool John Moores University, 146 Brownlow Hill, Liverpool L3 5RF, UK

³ Cahill Center for Astronomy and Astrophysics, California Institute of Technology, Mail Code 249-17, Pasadena, CA 91125, USA

⁴ Center for Interdisciplinary Exploration and Research in Astrophysics (CIERA), 1800 Sherman Avenue, Evanston, IL 60201, USA

⁵ Department of Astronomy, Oskar Klein Center, Stockholm University, SE-106 91 Stockholm, Sweden

⁶ Department of Physics and Astronomy, University of North Carolina at Chapel Hill, Chapel Hill, NC 27599-3255, USA

⁷ DIRAC Institute, Department of Astronomy, University of Washington, 3910 15th Avenue NE, Seattle, WA 98195, USA

⁸ Department of Astronomy, University of California, Berkeley, CA 94720-3411, USA

⁹ Caltech Optical Observatories, California Institute of Technology, Pasadena, CA 91125, USA

¹⁰ School of Physics & Astronomy and Institute of Gravitational Wave Astronomy, University of Birmingham, UK

¹¹ Division of Physics, Mathematics and Astronomy, California Institute of Technology, Pasadena, CA 91125, USA

¹² IPAC, California Institute of Technology, 1200 East California Boulevard, Pasadena, CA 91125, USA

¹³ University Observatory, Faculty of Physics, Ludwig-Maximilians-Universität, Scheinerstr. 1, 81679 Munich, Germany

¹⁴ Excellence Cluster ORIGINS, Boltzmannstr. 2, 85748 Garching, Germany

¹⁵ McWilliams Center for Cosmology and Astrophysics, Department of Physics, Carnegie Mellon University, 5000 Forbes Avenue, Pittsburgh, PA 15213, USA

¹⁶ Center for Data Driven Discovery, California Institute of Technology, Pasadena, CA 91125, USA

¹⁷ Department of Physics and Astronomy, Northwestern University, 2145 Sheridan Road, Evanston, IL 60208, USA

¹⁸ NSF-Simons AI Institute for the Sky (SkAI), 172 East Chestnut Street, Chicago, IL 60611, USA

¹⁹ Institut für Physik, Humboldt-Universität zu Berlin, Newtonstr. 15, 12489 Berlin, Germany

²⁰ Department of Physics and Astronomy, UCLA PAB 430 Portola Plaza Los Angeles, CA 90095-1547, USA

Received 2025 October 28; revised 2025 November 7; accepted 2025 November 7; published 2025 December 5

Abstract

We present the discovery of SN 2025wny (ZTF25abnjznp/GOTO25gqt) and spectroscopic classification of this event as the first gravitationally lensed Type I superluminous supernova (SLSN-I). Deep ground-based follow-up observations resolve four images of the supernova with $\sim 1''7$ angular separation from the main lens galaxy, each coincident with the lensed images of a background galaxy seen in archival imaging of the field. Spectroscopy of the brightest image shows narrow features matching absorption lines at a redshift of $z = 2.010$ and broad features matching those seen in superluminous SNe with far-UV coverage. We infer a magnification factor of $\mu \sim 20\text{--}50$ for the brightest image in the system, based on photometric and spectroscopic comparisons to other SLSNe-I. SN 2025wny demonstrates that gravitationally lensed SNe are in reach of ground-based facilities out to redshifts far higher than previously assumed, and provide a unique window into studying distant supernovae and the internal properties of dwarf galaxies, as well as for time-delay cosmography.

Unified Astronomy Thesaurus concepts: [Gravitational lensing \(670\)](#); [Supernovae \(1668\)](#)

1. Introduction

Gravitationally lensed supernovae (glSNe) provide unique laboratories for both astrophysics and cosmology, offering direct probes of galaxy-scale mass distributions and independent measurements of the Hubble constant, H_0 , through time-delay cosmography (S. Refsdal 1964). Over the past decade, the number of known lensed SNe has grown from single prototypes to a small but diverse sample spanning multiple SN types and redshifts. The first gravitationally lensed SN to be detected, PS1-10afx, was identified serendipitously and first suggested to be an exotic type of superluminous supernova (R. Chornock

et al. 2013), before R. M. Quimby et al. (2013) demonstrated it was in fact a highly magnified normal Type Ia SN. The event had faded before multiple images could be resolved. The first multiply imaged SN discovered, S. Refsdal, revealed multiple images of the same explosion due to deflection by a galaxy cluster lens (P. L. Kelly et al. 2015, 2016). The first resolved multiply imaged Type Ia SN, iPTF16geu, was found in a galaxy-scale lens system and demonstrated the power of wide-field time-domain surveys to uncover such rare events (A. Goobar et al. 2017). Subsequent discoveries have expanded this class, including the strongly magnified SN Zwicky (A. Goobar et al. 2023) and additional examples uncovered through systematic searches with the Hubble Space Telescope (HST) and JWST (S. A. Rodney et al. 2021; B. L. Frye et al. 2024; J. D. R. Pierel et al. 2024). The challenges of ground-based strongly lensed SN searches are discussed in A. Goobar



Original content from this work may be used under the terms of the [Creative Commons Attribution 4.0 licence](#). Any further distribution of this work must maintain attribution to the author(s) and the title of the work, journal citation and DOI.

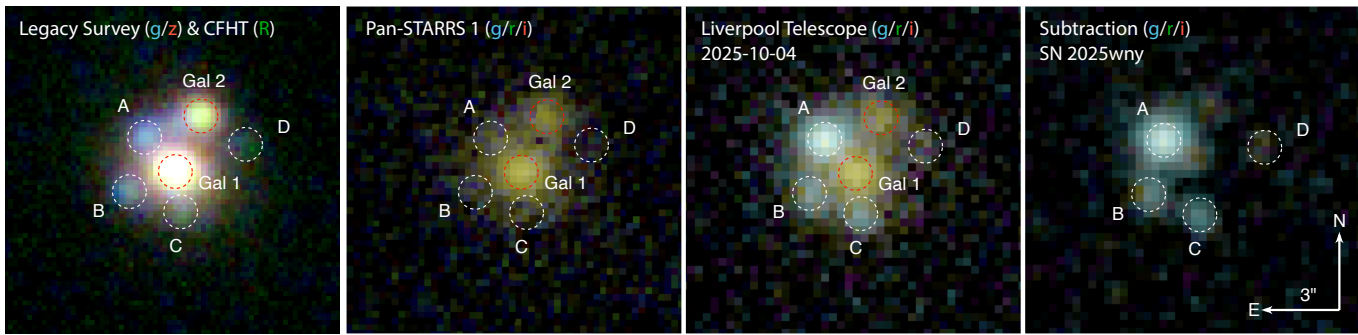


Figure 1. RGB composite images of the lens system from Legacy Survey (g - and z -bands) and CFHT R -band imaging (left panel) prior to the SN explosion. The following panels show the Pan-STARRS images used for image subtraction (center left), LT gri images from 2025 October 4 (center right), and the four lensed images of SN 2025wny after subtraction of the reference image (right panel).

et al. (2025), and many of the science potentials are highlighted in the review by S. H. Suyu et al. (2024).

Because of line blanketing and photospheric cooling, most SNe emit little UV luminosity after the first few days of explosion (P. J. Brown et al. 2009) and are thus difficult to detect and study at distances substantially beyond $z > 1$ in the optical band, even when gravitationally lensed. As a result, higher- z lensing systems have remained largely the domain of space telescopes with sensitive near-infrared capabilities (the Hubble Space Telescope and James Webb Space Telescope), which have found many distant SNe—typically behind known lensing clusters—but rarely classify them spectroscopically (e.g., D. Rubin et al. 2018; W. Chen et al. 2022; H. Yan et al. 2025).

In this Letter we report the discovery of SN 2025wny at $z = 2.010$, a Type I superluminous supernova (SLSN-I) that is strongly lensed and multiply imaged by a foreground galaxy at $z = 0.375$. It is the first known lensed SLSN, and the first SN of any type for which multiple images can be separately resolved in seeing-limited images from the ground. This event adds to the growing sample of gravitationally lensed transients and hugely expands the redshift horizon for ground-based lensing studies. It will provide new opportunities to constrain the lens potential, measure time delays for cosmography, and explore the properties of a high- z SN magnified by gravitational lensing in tandem with its star-forming dwarf host galaxy.

2. Observations

2.1. Discovery of SN 2025wny

SN 2025wny was first identified by the Zwicky Transient Facility (ZTF; E. C. Bellm et al. 2019; D. A. Duev et al. 2019; M. J. Graham et al. 2019; A. Mahabal et al. 2019; F. J. Masci et al. 2019; M. T. Patterson et al. 2019; R. Dekany et al. 2020) as a candidate transient on 2025 August 29 UT and given the identifier ZTF25abnjznp; forced photometry on recent images recovered prior detections dating back to 2025 August 27. It was reported to the Transient Name Server by the Gravitational-wave Optical Transient Observer (GOTO) on 2025 September 1 UT as GOTO25gqt (D. O’Neill et al. 2025).

The event was identified as a candidate of interest within a day of discovery during our daily screening of new transients crossmatched against public spectroscopic and photometric redshift catalogs.²¹ In this case, the transient was nearby in

projection to a massive luminous red galaxy (LRG) with an archival spectrum from the Dark Energy Spectroscopic Instrument (DESI), placing the redshift at $z = 0.3754 \pm 0.0001$ (DESI Collaboration et al. 2025). The brightness of the object was inconsistent with a Type Ia SN at the redshift of the galaxy, indicating that a background source with substantial lensing magnification was viable.

In addition to the DESI redshift, the transient was also flagged as lying $1''0$ from the known lens candidate PS1J0716+3821 (R. Cañameras et al. 2020) by our daily crossmatching to the Strong Lensing Database (SLED²²) of confirmed and candidate gravitational lenses, providing further support that SN 2025wny could be lensed.

Legacy Survey imaging (A. Dey et al. 2019) of the field shows a second red galaxy nearby, likely at the same redshift. Archival Canada–France–Hawaii Telescope (CFHT) imaging (S. D. J. Gwyn 2008) shows four images of a blue background object in a cross pattern around the LRGs and possible arc-like structures close to the brightest image. (A colorized image combining Legacy Survey and CFHT imaging is shown in the leftmost panel of Figure 1, with the four candidate images labeled A–D.)

2.2. Imaging

ZTF carried out regular survey observations of the field containing SN 2025wny starting 11 days prior to the time of discovery, which were processed according to the ZTF standard pipeline (F. J. Masci et al. 2019). The public photometry is presented here and is available via all public ZTF brokers.

Imaging observations with the IO:O camera on the Liverpool Telescope (LT) began on 2025 September 2 UT, as soon as the potential lensing nature of the system was identified. These initial exposures, and others on subsequent nights, showed a clear detection of a point source at the location of Image A, but due to the relatively short integration time, no other high signal-to-noise ratio (S/N) sources are apparent in the image or a difference subtraction of reference imaging in the same bands from Pan-STARRS 1 (K. C. Chambers et al. 2016). However, improved conditions on 2025 September 20 and on several subsequent nights revealed multiple clear detections of three residual sources (and a marginal detection of a fourth) in the subtraction image in an Einstein cross pattern, with locations consistent with the four candidate

²¹ Fritz/Skyportal was used to facilitate source crossmatching, data sharing, and exploratory analysis (S. J. van der Walt et al. 2019; M. W. Coughlin et al. 2023).

²² A cone search of $50''$ of the SLED database: <https://sled.amnh.org/>.

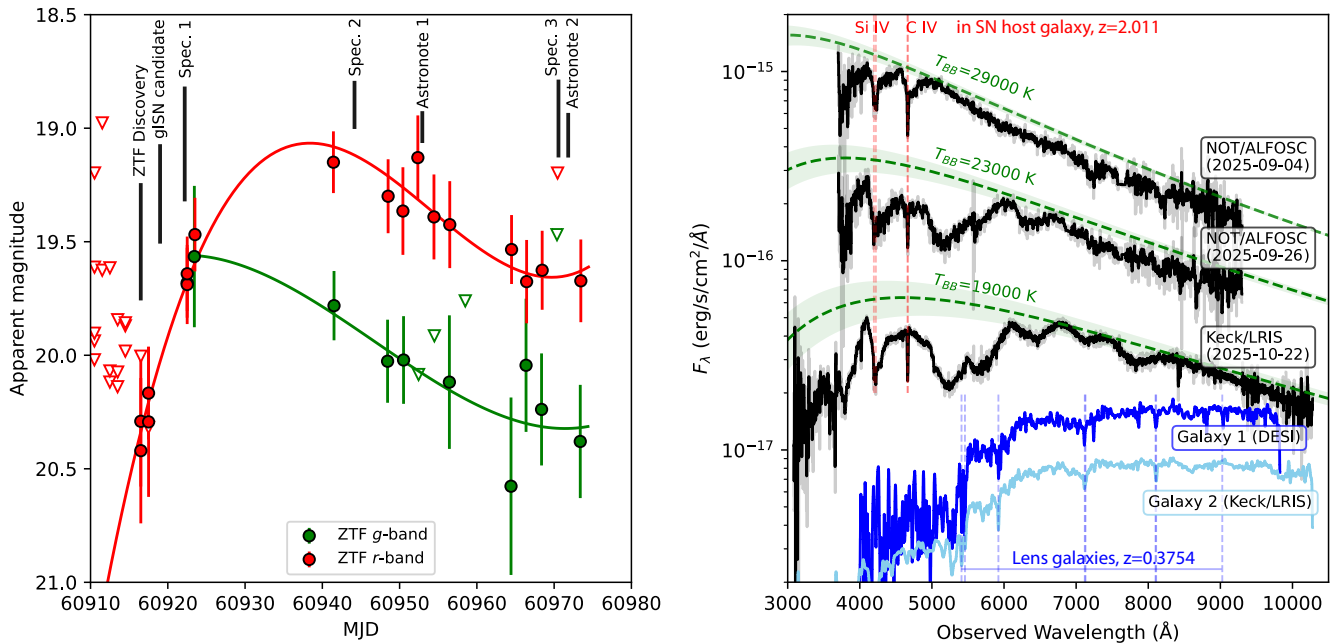


Figure 2. Left panel: public ZTF g - and r -band light curves of SN 2025wny, shown as green and red symbols. Black vertical lines indicate the time of the discovery, spectroscopic observations, and our reported AstroNotes (J. Johansson et al. 2025; J. Wise et al. 2025). Right panel: spectra of SN 2025wny (black lines) and the two galaxies forming the lens system (blue lines). The spectra have been offset for clarity. Prominent absorption lines from the SN host galaxy at $z = 2.010$, and the two lens galaxies at $z_{\text{lens}} = 0.375$, are marked with vertical red and blue lines, respectively. The dashed green curves show blackbody fits to the SN spectra, with $T_{BB} \sim 29,000, 23,000$, and $19,000$ K, for the three spectra.

galaxy-lens images in the CFHT images, a result we reported to the community as an AstroNote (J. Wise et al. 2025). Figure 1 shows red, green, and blue (RGB) false-color images of preexplosion data (left panels), postexplosion LT imaging, and the resulting subtraction image (right panels). From our observations on 2025 October 4 UT, we measure the brightest SN image (A) to have magnitudes of $g = 20.42 \pm 0.04$, $r = 19.60 \pm 0.03$, and $i = 19.54 \pm 0.03$.

Additional imaging observations from the Liverpool Telescope, the Palomar 60 inch Telescope, the Fraunhofer Telescope at Wendelstein Observatory, and other facilities will be presented in future work.

2.3. Spectroscopy

Three spectra of SN 2025wny are presented in this work:²³ two obtained using the Alhambra Faint Object Spectrograph and Camera (ALFOSC) on the 2.56 m Nordic Optical Telescope (NOT) on 2025 September 4 and 26 UT, and one with the Low-Resolution Imaging Spectrometer (LRIS; J. B. Oke et al. 1995) on the Keck I telescope on 2025 October 22 UT.

The NOT/ALFOSC spectra were obtained with a $1''$ wide slit using Grism 4. We reduced the spectra with a custom fork of PyPeIt (J. X. Prochaska et al. 2020a, 2020b), following standard procedures for preprocessing, 1D extraction, wavelength calibration, and flux calibration.

The Keck/LRIS observations were obtained with a $1''$ wide slit using the B400/3400 grism and R400/8500 grating at a position angle of 164° (covering images A and B, 45° away from the parallactic angle) as well as additional spectra

at other slit orientations covering other SN images and galaxy 2 (spectrum shown in Figure 2). Two exposures of 600 s were taken at each slit position. Spectra were reduced and extracted using LPipe (D. A. Perley 2019).

The first NOT spectrum (Figure 2) was almost entirely featureless except for a narrow absorption line at 4664 \AA and a possibly broader absorption feature at 4178 \AA . By the time of the second spectrum two weeks later, clear broad SN-like features had developed in the blue half of the spectrum, although these did not match any optical SN spectral templates.

The LRIS observation revealed numerous additional narrow absorption lines matching strong intergalactic/interstellar features at a common redshift of $z = 2.0104 \pm 0.0005$, establishing the redshift of the event. (The narrow line at 4664 \AA previously seen in the NOT spectra was one such feature, the C IV $\lambda\lambda 1550$ doublet.) Comparing the spectrum to UV templates, the broader features in the spectrum were found to match SLSNe-I, as reported by J. Johansson et al. (2025). More details on the spectral analysis are provided in Section 3.

3. Spectral Analysis

A comparison between the LRIS spectrum of SN 2025wny and rest-frame UV spectra of three superluminous supernovae is shown in Figure 3. The comparison events are SN 2016eay and SN 2017egm (two nearby SLSNe-I observed with HST; T. Kangas et al. 2017; L. Yan et al. 2017, 2018) and DES16C2nm (a SLSN-I at $z = 1.998$ that is not strongly lensed; M. Smith et al. 2018). All four spectra were taken shortly after the rest-frame near-UV peak of the light curve (Section 4). The locations of the broad absorption troughs seen in SN 2025wny match similar features in all three comparison objects, and can be attributed to various metals (primarily C, Mg, Si, Ti, and Fe), as in previous studies of SLSNe-I

²³ Additional spectra were acquired with the Next Generation Palomar Spectrograph on the Palomar 5 m Hale telescope, with the Kait Spectrograph on the Lick 3 m Shane telescope, and with the Spectral Energy Distribution Machine on P60; these spectra will be presented in future work.

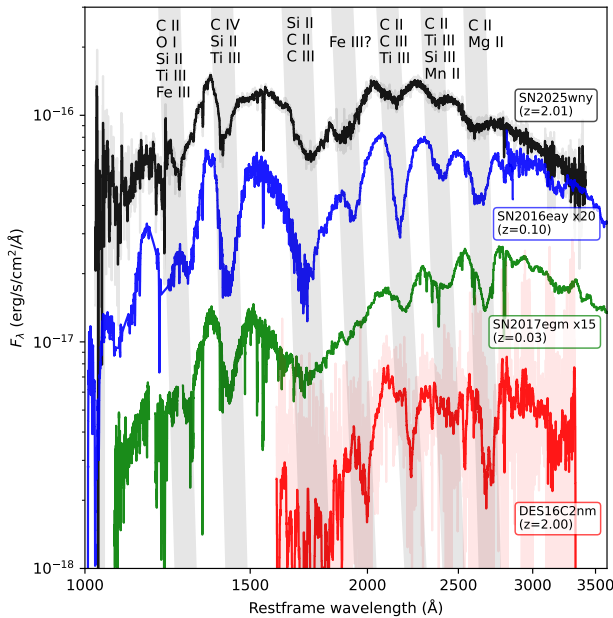


Figure 3. Keck/LRIS spectrum of SN 2025wny (black line) compared to HST spectra of the low- z SLSNe-I 2016eay (a.k.a Gaia16apd; blue line) and SN 2017egm (green line) and a Magellan/LDSS3 spectrum of high- z DES16C2nm (red line). All spectra are scaled by their luminosity distance relative to SN 2025wny, and for clarity SNe 2016eay and 2017egm have been offset by multiplicative factors of 20 and 15, respectively.

(R. M. Quimby et al. 2018). The spectra were not good matches to other potential UV-luminous transient classes (e.g., TDEs, SLSNe-II, or QSOs). This, combined with the blue colors, establishes SN 2025wny as a SLSN-I.

While the spectrum of SN 2025wny resembles that of SLSNe-I, it exhibits a bluer continuum than any of the comparison objects and the absorption features are generally weaker, with broader profiles. To some extent this could result from differences in observational phase, but it may also indicate differences in the chemical or ionization state of the ejecta. Fitted blackbody temperatures (using the rest-frame near-UV only to avoid line blanketing; see right panel of Figure 2) range from 29,000 to 19,000 K, with an uncertainty of ~ 1000 K. This is somewhat higher than the 14,000–17,000 K inferred from spectral fitting of other SLSNe with UV spectra (L. Yan et al. 2017).

The spectrum also shows a rich series of narrow absorption lines associated with absorption from the host galaxy. Figure 4 shows the spectrum after division by a continuum normalization model, with key detected features including H I $\lambda 1216$ ($\text{Ly}\alpha$), Si II $\lambda 1260$, C II $\lambda 1335$, Si IV $\lambda\lambda 1394, 1403$, Si II $\lambda 1527$, C IV $\lambda\lambda 1548, 1551$, and Mg II $\lambda\lambda 2796, 2803$.

We also note tentative detections of the Si II* $\lambda 1265$ and $\lambda 1533$ fine-structure transitions, possibly excited by the strong UV emission from the SN (E. Berger et al. 2006; J. X. Prochaska et al. 2006; P. M. Vreeswijk et al. 2007).

While a detailed study of the narrow absorption lines from the host system is beyond the scope of this analysis, we note that their strengths are relatively weak compared to what has been seen in other high-redshift absorption systems. Mg II $\lambda\lambda 2800$ is detected with equivalent width comparable to what has been seen in other SLSNe, but most other lines are weaker and the Fe II $\lambda 2344, 2383, 2600$ series commonly seen in gamma-ray burst (GRB) afterglow spectra (J. Selsing et al. 2019) is only marginally detected. We extracted equivalent

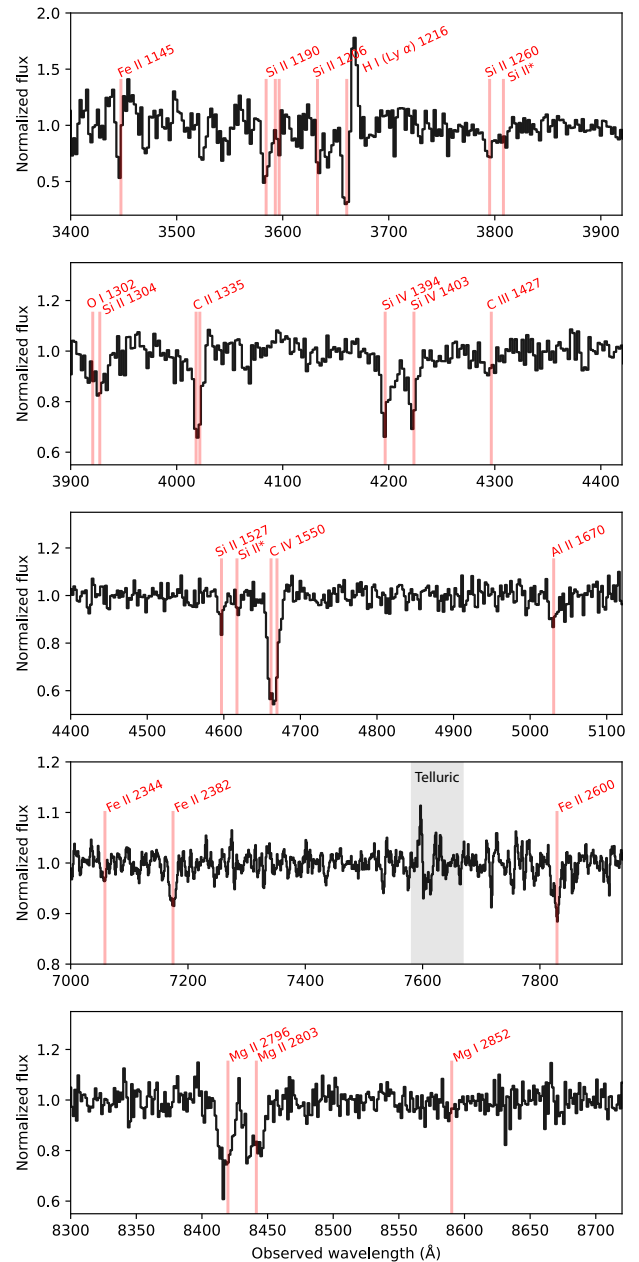


Figure 4. Selection of absorption lines identified in the Keck/LRIS spectrum of SN 2025wny, used to determine the SN host redshift ($z = 2.0104 \pm 0.0005$).

widths of the features marked on Figure 4 and used these to compute the mean line-strength parameter (LSP) of A. de Ugarte Postigo et al. (2012). We measure $\text{LSP} = -0.64$, placing the absorption strength at the 20th percentile of the GRB distribution.

A particularly notable case is the $\text{Ly}\alpha$ line: the profile of this line shows no damped wings and is consistent with being unresolved at the resolution of the spectrograph. This implies that the neutral hydrogen column is quite low: a conservative upper limit from fitting a Voigt profile is $\log_{10}(N_{\text{H}}/\text{cm}^{-2}) < 19.3$, which is already less than all but a few of the lowest- N_{H} GRB sightlines (N. R. Tanvir et al. 2019) and essentially all low- z star-forming galaxies for which a $\text{Ly}\alpha$ absorption measurement has been possible (J. H. McKinney et al. 2019; V. P. Kulkarni et al. 2022). A narrow $\text{Ly}\alpha$ emission component is also detected in the spectrum of SN 2025wny just redward of the absorption feature,

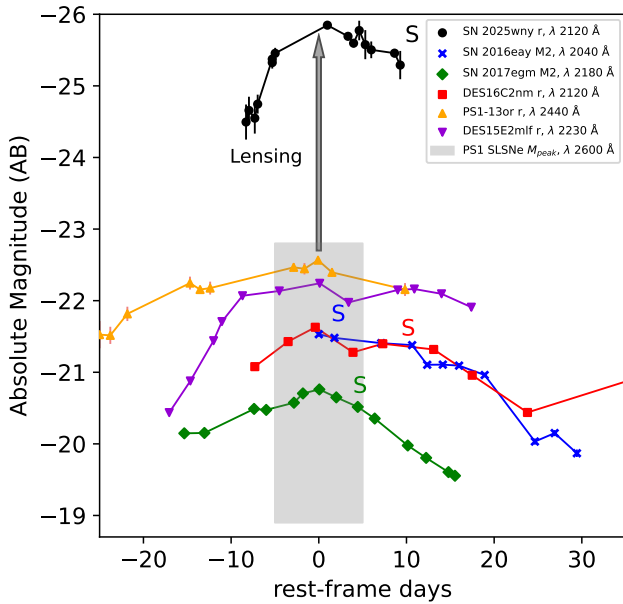


Figure 5. Rest-frame UV light curve of image A of SN 2025wny (from the ZTF r -band) compared to a set of comparison SLSN curves in similar rest-frame bands: SN 2017egm, SN 2016eay, PS1-13or, DES15E2mlf, and DES16C2nm. The observation times of the spectra used for the comparison in Figure 3 are marked with an “S”.

likely originating from star formation in the host. Taken together, these characteristics imply a low-mass, star-forming host galaxy with low neutral gas content and/or metallicity.

No strong absorption features from the $z = 0.375$ lensing galaxies are evident in the spectrum of Image A. This is not unexpected, given the relatively large impact parameter (~ 9 kpc projected), which probes the outer halo of the lens where column densities are low, and therefore does not require the lens to be unusually metal-poor.

4. Light Curve Analysis and Magnification

The r -band light curve from ZTF is presented again in Figure 5. The vertical axis shows the rest-frame absolute magnitude at the equivalent rest-frame central wavelength ($\lambda = 2120 \text{ \AA}$) with correction for Galactic extinction (E. F. Schlafly & D. P. Finkbeiner 2011) but no correction for host extinction or lensing magnification. For comparison, the host-subtracted Swift Ultraviolet-Optical Telescope (UVOT; P. W. A. Roming et al. 2005) light curves²⁴ of two low- z SLSNe (SN 2016eay at $z = 0.102$ and SN 2017egm at $z = 0.031$) are also shown in the approximately matching $UVM2$ filter. Also shown are a few examples of very luminous SNe found at higher redshift in deeper surveys, similarly matched by rest-frame central wavelength: PS1-13or from R. Lunnan et al. (2018), DES15E2mlf from Y.-C. Pan et al. (2017), and DES16C2nm from M. Smith et al. (2018). The gray box indicates the range of peak luminosities standardized at a (slightly redder) wavelength of $\lambda = 2600 \text{ \AA}$ from R. Lunnan et al. (2018).

Because of time dilation, the two-month period between the discovery of SN 2025wny and the most recent data corresponds to only 20 days in the rest frame, so only a limited time span is available to characterize its evolution. The rise of

1.5 mag over the first 10 rest-frame days is relatively steep for a SLSN (although not unprecedented: the light curve of DES15E2mlf shows similar behavior).

At a redshift of $z = 2.010$, the peak absolute magnitude of the SN without lensing correction is approximately -25.8 at $\lambda_{\text{rest}} = 2120 \text{ \AA}$. If SN 2025wny is intrinsically of similar luminosity and host extinction to a “typical” low- z SLSN (such as SN 2016eay), it would require a lensing magnification of ~ 4.3 mag (factor $\mu \sim 50$). Comparing instead to PS1-13or, the most UV-luminous event in the Pan-STARRS sample of R. Lunnan et al. (2018), would still require a magnification of ~ 3.2 mag ($\mu \sim 20$).

We infer that at least one, and possibly all, of the following are true: (a) the magnification factor of the system is very large ($\mu \gtrsim 20$, and possibly as much as $\mu \sim 50$); (b) in addition to being lensed, SN 2025wny was a particularly overluminous SLSN in the ultraviolet; or (c) SN 2025wny was discovered and observed in the rest-frame UV at an earlier phase than is normally possible for these events, and the early temperatures and UV luminosities for some SLSNe are higher than previously anticipated. Future observations and analysis will help to distinguish these possibilities.

5. Conclusions

The discovery of SN 2025wny underscores the accelerating pace with which lensed supernovae are being found, marking the transition from rare, serendipitous detections to an emerging population accessible through systematic time-domain surveys. Over the next decade, this field is poised for rapid growth. The Vera C. Rubin Observatory’s Legacy Survey of Space and Time (LSST) will transform the landscape of lensed transient discovery, with forecasts predicting several tens of multiply imaged SNe per year across a broad range of redshifts and environments (e.g., D. A. Goldstein et al. 2019; R. Wojtak et al. 2019; N. Arendse et al. 2024; A. Sainz de Murieta et al. 2024). LSST’s depth, cadence, and photometric stability will enable the detection of faint, highly magnified events, while its extensive sky coverage will provide the statistical foundation for testing models of galaxy mass distributions and cosmological parameters.

At the same time, space-based missions such as JWST, Euclid, and Roman will provide complementary imaging and spectroscopy crucial for time-delay measurements, host-galaxy characterization, and high-resolution lens modeling. In particular, JWST/NIRSpec and NIRCams observations can yield precise phase-resolved spectra and astrometry of individual SN images, such observations, along with HST imaging in the optical are scheduled for SN 2025wny (PI: Goobar). In the longer term, Euclid’s wide-area lens catalog will greatly expand the pool of candidate deflectors (T. E. Collett 2015). Together with ongoing efforts by ground-based facilities, this synergy will enable routine discovery and detailed study of lensed SNe, bridging the gap between current pilot samples and the statistically powerful datasets required for cosmology.

As analysis techniques continue to mature—incorporating forward modeling, simulation-based inference, and improved microlensing treatments—lensed SNe are expected to evolve from curiosities to precision probes of both lens physics and cosmic expansion. The discovery of SN 2025wny thus represents not only an individual milestone but also a glimpse into a rapidly unfolding era of time-delay cosmography powered by the next generation of time-domain surveys.

²⁴ UVOT light curves were built directly using data from the Swift archive using HEASoft 6.30.

In addition to underscoring the utility of lensed superluminous supernovae as cosmological probes, the discovery of SN 2025wny also opens up a new pathway for the use of these events to study galaxy evolution. While the potential for very luminous supernovae to serve as probes of high- z dwarf galaxies was realized shortly after the discovery of the first few events at $z > 1$ (E. Berger et al. 2012), in practice SLSNe have rarely been able to serve this purpose due to the large amounts of telescope time required to obtain meaningful S/N beyond $z > 1$. While the observations reported here do not yet permit a detailed analysis of the host environment, deeper observations with higher-resolution instruments would permit constraints on the metallicity and kinematics of the host interstellar medium that could then be complemented by detailed late-time observations of the (also magnified) host itself, providing an unprecedented view into the nature of a distant star-forming galaxy in both absorption and emission.

Acknowledgments

We thank Stefan Taubenberger for sharing the HOLISMOKES team’s pre-submission draft on this object (S. Taubenberger et al. 2025), following our AstroNote on the classification of SN 2025wny.

A.G. acknowledges support from the Swedish Research Council through project Dnr 2020-03444 and the Swedish National Space Agency, Dnr 2023-00226.

C.L. acknowledges funding from the European Union’s Horizon Europe research and innovation programme under the Marie Skłodowska-Curie grant agreement No. 101105725.

A.G. acknowledges financial support from the research project grant “Understanding the Dynamic Universe” funded by the Knut and Alice Wallenberg under Dnr KAW 2018.0067, Vetenskapsrådet, the Swedish Research Council through grants project Dnr 2020-03444, the G.R.E.A.T re- search environment, Dnr 2016-06012, and the Swedish National Space Agency, Dnr 2023-00226.

S.D. acknowledges support from UK Research and Innovation (UKRI) under the UK government’s Horizon Europe funding Guarantee EP/Z000475/1.

E.M. acknowledges support from the Swedish Research Council under Dnr VR 2024-03927.

A.A.M. is supported by DoE award # DE-SC0025599 to Northwestern University and by Cottrell Scholar Award # CS-CSA-2025-059 from Re- search Corporation for Science Advancement.

Funded in part by the Deutsche Forschungsgemeinschaft (DFG, German Research Foundation) under Germany’s Excellence Strategy – EXC-2094 – 390783311.

Funded by the European Union (ERC, project number 101042299, TransPIre).

Based on observations obtained with the 48 inch Samuel Oschin Telescope and the 60 inch Telescope at the Palomar Observatory as part of the Zwicky Transient Facility project. ZTF is supported by the National Science Foundation under Award 2407588 and a partnership including Caltech, USA; Caltech/IPAC, USA; University of Maryland, USA; University of California, Berkeley, USA; University of Wisconsin at Milwaukee, USA; Cornell University, USA; Drexel University, USA; University of North Carolina at Chapel Hill, USA; Institute of Science and Technology, Austria; National Central University, Taiwan; and OKC, University of Stockholm, Sweden. Operations are conducted by Caltech’s

Optical Observatory (COO), Caltech/IPAC, and the University of Washington at Seattle, USA.

The Liverpool Telescope is operated on the island of La Palma by Liverpool John Moores University in the Spanish Observatorio del Roque de los Muchachos of the Instituto de Astrofísica de Canarias with financial support from the UK Science and Technology Facilities Council.

Based on observations made with the Nordic Optical Telescope, owned in collaboration by the University of Turku and Aarhus University, and operated jointly by Aarhus University, the University of Turku, and the University of Oslo, representing Denmark, Finland, and Norway, the University of Iceland, and Stockholm University at the Observatorio del Roque de los Muchachos, La Palma, Spain, of the Instituto de Astrofísica de Canarias. The NOT data were obtained under program ID P70-501.

Some of the data presented herein were obtained at the W. M. Keck Observatory, which is operated as a scientific partnership among the California Institute of Technology, the University of California, and NASA. The Observatory was made possible by the generous financial support of the W. M. Keck Foundation. The authors wish to recognize and acknowledge the very significant cultural role and reverence that the summit of Maunakea has always had within the indigenous Hawaiian community. We are most fortunate to have the opportunity to conduct observations from this mountain.

Facilities: Keck:I (LRIS), NOT (ALFOSC), Liverpool:2m, PO:1.2m.

Software: Astropy (Astropy Collaboration et al. 2013, 2018, 2022), Matplotlib (J. D. Hunter 2007).

ORCID iDs

Joel Johansson  <https://orcid.org/0000-0001-5975-290X>
 Daniel A. Perley  <https://orcid.org/0000-0001-8472-1996>
 Ariel Goobar  <https://orcid.org/0000-0002-4163-4996>
 Jacob L. Wise  <https://orcid.org/0000-0003-0733-2916>
 Yu-Jing Qin  <https://orcid.org/0000-0003-3658-6026>
 Zoë McGrath  <https://orcid.org/0009-0006-0726-1328>
 Steve Schulze  <https://orcid.org/0000-0001-6797-1889>
 Cameron Lemon  <https://orcid.org/0000-0003-2456-9317>
 Anjasha Gangopadhyay  <https://orcid.org/0000-0002-3884-5637>
 Konstantinos Tsalapatas  <https://orcid.org/0009-0004-1062-8886>
 Igor Andreoni  <https://orcid.org/0000-0002-8977-1498>
 Eric C. Bellm  <https://orcid.org/0000-0001-8018-5348>
 Joshua S. Bloom  <https://orcid.org/0000-0002-7777-216X>
 Richard Dekany  <https://orcid.org/0000-0002-5884-7867>
 Suhail Dhawan  <https://orcid.org/0000-0002-2376-6979>
 Claes Fransson  <https://orcid.org/0000-0001-8532-3594>
 Christoffer Fremling  <https://orcid.org/0000-0002-4223-103X>
 Matthew J. Graham  <https://orcid.org/0000-0002-3168-0139>
 Steven L. Groom  <https://orcid.org/0000-0001-5668-3507>
 Daniel Gruen  <https://orcid.org/0000-0003-3270-7644>
 Xander J. Hall  <https://orcid.org/0000-0002-9364-5419>
 George Helou  <https://orcid.org/0000-0003-3367-3415>
 Mansi Kasliwal  <https://orcid.org/0000-0002-5619-4938>
 Russ R. Laher  <https://orcid.org/0000-0003-2451-5482>
 Ragnhild Lunnan  <https://orcid.org/0000-0001-9454-4639>
 Ashish A. Mahabal  <https://orcid.org/0000-0003-2242-0244>
 Adam A. Miller  <https://orcid.org/0000-0001-9515-478X>
 Edvard Mörtzell  <https://orcid.org/0000-0002-8380-6143>

Jakob Nordin  <https://orcid.org/0000-0001-8342-6274>
 Jacob Osman Hjortlund  <https://orcid.org/0009-0009-6243-8300>
 R. Michael Rich  <https://orcid.org/0000-0003-0427-8387>
 Reed L. Riddle  <https://orcid.org/0000-0002-0387-370X>
 Avinash Singh  <https://orcid.org/0000-0003-2091-622X>
 Jesper Sollerman  <https://orcid.org/0000-0003-1546-6615>
 Alice Townsend  <https://orcid.org/0000-0001-6343-3362>
 Lin Yan  <https://orcid.org/0000-0003-1710-9339>

References

- Arendse, N., Dhawan, S., Sagués Carracedo, A., et al. 2024, *MNRAS*, **531**, 3509
- Astropy Collaboration, Price-Whelan, A. M., Lim, P. L., et al. 2022, *ApJ*, **935**, 167
- Astropy Collaboration, Price-Whelan, A. M., Sipőcz, B. M., et al. 2018, *AJ*, **156**, 123
- Astropy Collaboration, Robitaille, T. P., Tollerud, E. J., et al. 2013, *A&A*, **558**, A33
- Bellm, E. C., Kulkarni, S. R., Graham, M. J., et al. 2019, *PASP*, **131**, 018002
- Berger, E., Chornock, R., Lunnan, R., et al. 2012, *ApJL*, **755**, L29
- Berger, E., Penprase, B. E., Cenko, S. B., et al. 2006, *ApJ*, **642**, 979
- Brown, P. J., Holland, S. T., Immler, S., et al. 2009, *AJ*, **137**, 4517
- Cañameras, R., Schuldt, S., Suyu, S. H., et al. 2020, *A&A*, **644**, A163
- Chambers, K. C., Magnier, E. A., Metcalfe, N., et al. 2016, arXiv:1612.05560
- Chen, W., Kelly, P. L., Oguri, M., et al. 2022, *Natur*, **611**, 256
- Chornock, R., Berger, E., Rest, A., et al. 2013, *ApJ*, **767**, 162
- Collett, T. E. 2015, *ApJ*, **811**, 20
- Coughlin, M. W., Bloom, J. S., Nir, G., et al. 2023, *ApJS*, **267**, 31
- de Ugarte Postigo, A., Fynbo, J. P. U., Thöne, C. C., et al. 2012, *A&A*, **548**, A11
- Dekany, R., Smith, R. M., Riddle, R., et al. 2020, *PASP*, **132**, 038001
- DESI Collaboration, Abdul-Karim, M., Adame, A. G., et al. 2025, arXiv:2503.14745
- Dey, A., Schlegel, D. J., Lang, D., et al. 2019, *AJ*, **157**, 168
- Duev, D. A., Mahabal, A., Masci, F. J., et al. 2019, *MNRAS*, **489**, 3582
- Frye, B. L., Pascale, M., Pierel, J., et al. 2024, *ApJ*, **961**, 171
- Goldstein, D. A., Nugent, P. E., & Goobar, A. 2019, *ApJS*, **243**, 6
- Goobar, A., Amanullah, R., Kulkarni, S. R., et al. 2017, *Sci*, **356**, 291
- Goobar, A., Johansson, J., & Sagués Carracedo, A. 2025, *RSPTA*, **383**, 20240123
- Goobar, A., Johansson, J., Schulze, S., et al. 2023, *NatAs*, **7**, 1098
- Graham, M. J., Kulkarni, S. R., Bellm, E. C., et al. 2019, *PASP*, **131**, 078001
- Gwyn, S. D. J. 2008, *PASP*, **120**, 212
- Hunter, J. D. 2007, *CSE*, **9**, 90
- Johansson, J., Qin, Y., Goobar, A., et al. 2025, *TNSAN*, **306**, 1
- Kangas, T., Blagorodnova, N., Mattila, S., et al. 2017, *MNRAS*, **469**, 1246
- Kelly, P. L., Brammer, G., Selsing, J., et al. 2016, *ApJ*, **831**, 205
- Kelly, P. L., Rodney, S. A., Treu, T., et al. 2015, *Sci*, **347**, 1123
- Kulkarni, V. P., Bowen, D. V., Straka, L. A., et al. 2022, *ApJ*, **929**, 150
- Lunnan, R., Chornock, R., Berger, E., et al. 2018, *ApJ*, **852**, 81
- Mahabal, A., Rebbapragada, U., Walters, R., et al. 2019, *PASP*, **131**, 038002
- Masci, F. J., Laher, R. R., Rusholme, B., et al. 2019, *PASP*, **131**, 018003
- McKinney, J. H., Jaskot, A. E., Oey, M. S., et al. 2019, *ApJ*, **874**, 52
- Oke, J. B., Cohen, J. G., Carr, M., et al. 1995, *PASP*, **107**, 375
- O'Neill, D., Ramsay, G., Ackley, K., et al. 2025, *TNSTR*, **2025-3492**, 1
- Pan, Y.-C., Foley, R. J., Smith, M., et al. 2017, *MNRAS*, **470**, 4241
- Patterson, M. T., Bellm, E. C., Rusholme, B., et al. 2019, *PASP*, **131**, 018001
- Perley, D. A. 2019, *PASP*, **131**, 084503
- Pierel, J. D. R., Newman, A. B., Dhawan, S., et al. 2024, *ApJL*, **967**, L37
- Prochaska, J. X., Chen, H.-W., & Bloom, J. S. 2006, *ApJ*, **648**, 95
- Prochaska, J. X., Hennawi, J., Cooke, R., et al. 2020a, pypeit/PypeIt: Release v1.0.0, Zenodo, doi:10.5281/zenodo.3743493
- Prochaska, J. X., Hennawi, J. F., Westfall, K. B., et al. 2020b, *JOSS*, **5**, 2308
- Quimby, R. M., Cia, A. D., Gal-Yam, A., et al. 2018, *ApJ*, **855**, 2
- Quimby, R. M., Werner, M. C., Oguri, M., et al. 2013, *ApJL*, **768**, L20
- Refsdal, S. 1964, *MNRAS*, **128**, 307
- Rodney, S. A., Brammer, G. B., Pierel, J. D. R., et al. 2021, *NatAs*, **5**, 1118
- Roming, P. W. A., Kennedy, T. E., Mason, K. O., et al. 2005, *SSRv*, **120**, 95
- Rubin, D., Hayden, B., Huang, X., et al. 2018, *ApJ*, **866**, 65
- Sainz de Murieta, A., Collett, T. E., Magee, M. R., et al. 2024, *MNRAS*, **535**, 2523
- Schlafly, E. F., & Finkbeiner, D. P. 2011, *ApJ*, **737**, 103
- Selsing, J., Malesani, D., Goldoni, P., et al. 2019, *A&A*, **623**, A92
- Smith, M., Sullivan, M., Nichol, R. C., et al. 2018, *ApJ*, **854**, 37
- Suyu, S. H., Goobar, A., Collett, T., More, A., & Vernardos, G. 2024, *SSRv*, **220**, 13
- Tanvir, N. R., Fynbo, J. P. U., de Ugarte Postigo, A., et al. 2019, *MNRAS*, **483**, 5380
- Taubenberger, S., Acebron, A., Cañameras, R., et al. 2025, arXiv:2510.21694
- van der Walt, S. J., Crellin-Quick, A., & Bloom, J. S. 2019, *JOSS*, **4**, 1247
- Vreeswijk, P. M., Ledoux, C., Smette, A., et al. 2007, *A&A*, **468**, 83
- Wise, J., Perley, D., Goobar, A., Johansson, J., & McGrath, Z. 2025, *TNSAN*, **296**, 1
- Wojtak, R., Hjorth, J., & Gall, C. 2019, *MNRAS*, **487**, 3342
- Yan, H., Sun, B., Ma, Z., et al. 2025, arXiv:2506.12175
- Yan, L., Perley, D. A., De Cia, A., et al. 2018, *ApJ*, **858**, 91
- Yan, L., Quimby, R., Gal-Yam, A., et al. 2017, *ApJ*, **840**, 57